

# Monitoring Microalgae Population Growth by using Fe<sub>3</sub>O<sub>4</sub> Nanoparticles-based Surface Plasmon Resonance (SPR) Biosensor

D T Nurrohman<sup>1</sup>, M Oktivina<sup>1</sup>, E Suharyadi<sup>1</sup>, E A Suyono<sup>2</sup> and K Abraha<sup>1</sup>

<sup>1</sup>Department of Physics, Universitas Gadjah Mada, Indonesia

<sup>2</sup>Faculty of Biology, Universitas Gadjah Mada, Indonesia

Email : esuharyadi@ugm.ac.id

**Abstract.** The population growth of microalgae has been successfully monitored by using the surface plasmon resonance (SPR)-based biosensor activated by using PEG-4000 functionalized Fe<sub>3</sub>O<sub>4</sub> magnetic nanoparticles. The SPR-based biosensor in this work used Kretschmann configuration and He-Ne laser beam ( $\lambda = 633\text{nm}$ ). The population of microalgae were estimated by using calibration curve. The shift of SPR angle happens due to the change of dielectric medium from prism/Au/air system to prism/Au/Fe<sub>3</sub>O<sub>4</sub>+PEG+microalgae/cover glass system. The change of dielectric medium occurs due to deposition of Fe<sub>3</sub>O<sub>4</sub>+PEG+microalgae samples that were monitored for seven days. The population of microalgae on the first day was estimated of 1188146 cell/ml and SPR angle had shifted from 42.8° to 69.0°. The SPR angle shifted as much as 26.2°. The population of microalgae grew significantly on the third day as much as 1649106 cell/ml and the SPR angle had shifted 43.8° to 71.1°. The SPR angle shifted as much as 27.3°. On fourth to seventh day, the population of microalgae decreased. The population of microalgae on the seventh day was estimated of 1206961 cell/ml and the SPR angle had shifted from 44.0° to 68.8°. The SPR angle shifted as much as 24.8 degrees. The shift of SPR angle was influenced by the population of microalgae so that the SPR-based biosensor has the potential for use in monitoring the microalgae population.

**Keywords:** Surface Plasmon Resonance (SPR), Magnetic Fe<sub>3</sub>O<sub>4</sub> nanoparticle, Attenuated total reflection (ATR), Microalgae

## 1. Introduction

Surface plasmon resonance (SPR) is an optical sensing technique based on the electromagnetic phenomenon in which surface plasmon polaritons (SPP) waves are used to probe the interactions between target molecules and receptor molecules [1]. The interaction between target molecules and receptor molecules will produce a local change in the refractive index (RI) at the metal-dielectric interfaces. The RI change will then further affect the propagation constant of the SPPs which can be measured by a phenomenon termed as attenuated total reflection (ATR).

Surface plasmon resonance (SPR) appears as a sharp minimum (plasmon dip) in the internal reflectance of a metal film deposited on the face of a prism [2]. The position of plasmon dip can be monitored in term of incident angle versus reflectance interrogation. These approaches are capable of recognizing biological events on their sensing surfaces [3]. Today, SPR-based biosensors are increasingly not only in gas sensing [4], but also in many other important applications such as



detection of low levels of *Escherichia coli* [5], *Salmonella* [6], and sensing of living cells [7]. Another potential of SPR-based biosensor that may be applied is for monitoring the growth of microalgae.

During this time, determining the growth of microalgae is carried out by a direct calculation by using the hemocytometer. This method requires a long time and will be difficult when there is a lot of cells in the hemocytometer. Another device that can be used is UV-Vis spectrophotometer. However, this device is an additional tool only for avoiding repeated calculations by using the hemocytometer.

In this paper, an SPR-based biosensor has been developed for growth monitoring of microalgae population based on the shift of the plasmon dip at reflectivity graph.  $\text{Fe}_3\text{O}_4$  magnetic nanoparticles have been used in this study because of some of its unique properties (superparamagnetic properties, perfectly reacts with biomolecules and larger surface area).,  $\text{Fe}_3\text{O}_4$  nanoparticles must be functionalized by encapsulation using polyethylene glycol 4000(PEG-4000) to be able for binding microalgae. In this study, growth monitoring of microalgae population obtained from the shift of the plasmon dip at reflectivity graph is compared with the data obtained by using UV-Vis spectrophotometer.

## 2. Experimental Method

### 2.1 Deposition of Au thin layer on the prism

Pure gold (Au) with mass 15,4 mg was deposited on the surface of prism by evaporating it at pressure point of  $3 \cdot 10^{-3}$  Pa and an electric current of 50 A for 7 minutes. The prism-coated was then called prism/Au/air system.

### 2.2 Device set-up

SPR device set up consists of the He-Ne laser (OSK Ogawa Seiki Co Ltd,  $\lambda = 632.8$  nm), a polarizer, a beam splitter, two detectors (laser power meter) and a BK7 prism (Figure 1).

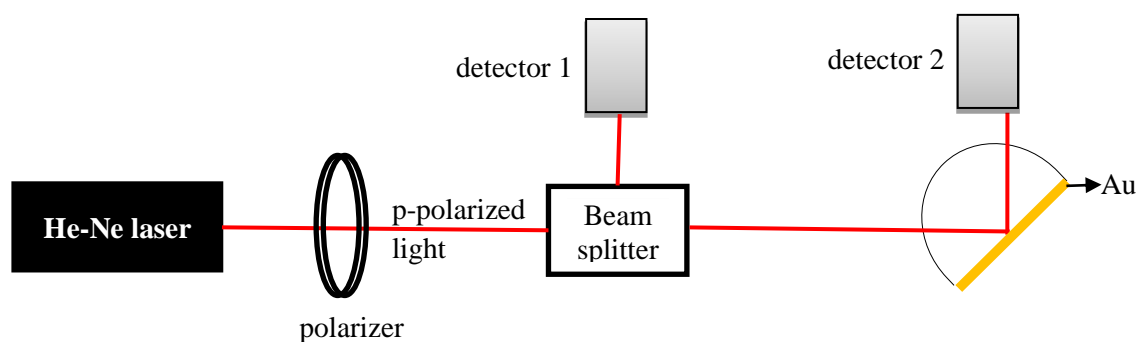


**Figure 1.** SPR set-up device in Kretschmann configuration.

Reflectivity graph of SPR was observed by varying the light incident angle ( $\theta$ ) within the angle range of  $30^\circ$  -  $80^\circ$  and recording the reflectivity ( $R$ ). Reflectivity in this experiment is defined by the power ratio recorded by detector 2 and detector 1. These values were plotted in a  $R$  vs  $\theta$  reflectivity graph.

### 2.3 $\text{Fe}_3\text{O}_4$ synthesis and functionality

$\text{Fe}_3\text{O}_4$  magnetic nanoparticles were synthesized by using co-precipitation method. Iron II sulfate heptahydrate with iron III chloride hexahydrate were dissolved in distilled water, and then the solution formed was titrated by 60 mL ammonia (with the ammonia concentration of 10%). The solution was stirred at a temperature of  $30^\circ\text{C}$  with the angular speed of 450 rpm for 90 min. After that, it was placed on the permanent magnet and washed with distilled water. The precipitated solution was dried at  $80^\circ\text{C}$  for 2 hours by using a furnace. Finally, it was ground to powder and kept in an air-tight container.

The functionality of Fe<sub>3</sub>O<sub>4</sub> nanoparticles was done with PEG applying the mass ratio of 1:1 for Fe<sub>3</sub>O<sub>4</sub> and PEG. Fe<sub>3</sub>O<sub>4</sub> and PEG were respectively dissolved in distilled water for 30 minutes, and then both solutions were mixed in a steady state in the stirrer for 1 hour. The solution that has been formed was dried to obtain Fe<sub>3</sub>O<sub>4</sub> nanoparticles that have been functionalized with PEG (Fe<sub>3</sub>O<sub>4</sub> + PEG).

#### 2.4 Microalgae culture

Glagah microalgae isolates were used in this study. This microalgae was isolated from the coast Glagah, Kulon Progo, Yogyakarta. The culture of microalgae is by Bold Basal Medium method (BBM). The culture medium is made in a laminar air flow (LAF) and sterilized by using an autoclave for 2 hours. Microalgae is inserted into a medium which has been sterilized and its growth was then observed. The growth of microalgae was monitored by using UV-Vis spectrophotometer (Thermo scientific Genesis 10uv Scanning) and SPR-based biosensors for seven days, each of them was in the intervals of 24 hours. The population of microalgae with UV-Vis spectrophotometer was determined by using a calibration curve.

#### 2.5 Calibration curve

Calibration curve gives the relationship between concentration and absorbance value. The number of cells for five samples of microalgae are calculated by using Haemocytometer Nuebauer of 1 mm to obtain the concentration value. The concentration of the number of cells from each sample was then determined by using Equation 2 as follows :

$$\text{Concentration} \left( \frac{\text{cell}}{\text{ml}} \right) = \text{number of cell} \times 5 \times 10^4 \quad (2)$$

Absorbance of each sample was then measured by using a UV-Vis spectrophotometer. After that, concentration and absorbance values were plotted to obtain a linear equation expressing their relation.

#### 2.6 Microalgae Deposition

Fe<sub>3</sub>O<sub>4</sub> + PEG were dissolved in distilled water for 30 minutes. The dispersed solution was then mixed with samples of microalgae that was being monitored. The sample is called as Fe<sub>3</sub>O<sub>4</sub> + PEG + microalgae sample. After that, this sample was deposited on prism/Au/air system by using a micropipette so that the prism system changed into prism/Au/Fe<sub>3</sub>O<sub>4</sub> + PEG + microalgae/cover glass system. The FTIR characterization was carried out on Fe<sub>3</sub>O<sub>4</sub>, PEG, Fe<sub>3</sub>O<sub>4</sub> + PEG and Fe<sub>3</sub>O<sub>4</sub> + PEG + microalgae samples to study the interaction between the the Fe<sub>3</sub>O<sub>4</sub> + PEG and microalgae.

### 3. Results and Discussion

#### 3.1 Interaction of Fe<sub>3</sub>O<sub>4</sub> + PEG with microalgae

The FTIR spectra of the samples are presented in Figure 2. The type of molecular vibration that occurs in the sample is shown in Table 1. The peaks located in 408.91 and 586.36 cm<sup>-1</sup> (in Figure 2a) are due to the stretching vibrations of Fe – O bonds in octahedral and tetrahedral sites [8]. The peak at 3433.29 cm<sup>-1</sup> is attributed to the stretching vibrations of –OH group [9]. In the Fe<sub>3</sub>O<sub>4</sub>+PEG sample (in Figure 2c), the peak of Fe-O bond has shifted from 408.91 to 401.19 cm<sup>-1</sup>. Besides that, the peak located in 2893.92 and 3448.72 cm<sup>-1</sup> are –OH group which indicates the presence of PEG in the Fe<sub>3</sub>O<sub>4</sub> nanoparticles. From this result, Fe<sub>3</sub>O<sub>4</sub>+PEG sample is strong evidence for the formation of PEG-coated nanoparticles.

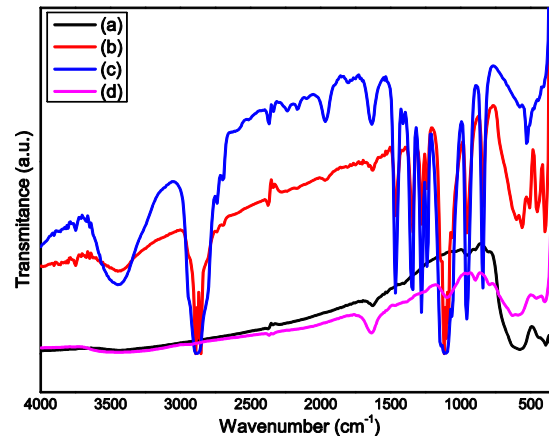


**Figure 2.** FTIR Spectra (a)  $\text{Fe}_3\text{O}_4$  (b) PEG (c)  $\text{Fe}_3\text{O}_4$ +PEG and (d)  $\text{Fe}_3\text{O}_4$ +PEG+microalgae.

In  $\text{Fe}_3\text{O}_4$ +PEG+microalgae samples, the peak at Fe – O in tetrahedral sites has the same peak with  $\text{Fe}_3\text{O}_4$ +PEG samples. This phenomenon indicates that  $\text{Fe}_3\text{O}_4$  nanoparticles have been successfully encapsulated by PEG and so there is no direct interaction between Fe – O in  $\text{Fe}_3\text{O}_4$  nanoparticles with microalgae. Besides that, the shift of absorption peak has occurred in C – O – C, C – O and  $\text{CH}_2$ . The shift of absorption peak in C – O – C and C – O bonds from the sample of  $\text{Fe}_3\text{O}_4$  + PEG and  $\text{Fe}_3\text{O}_4$  + PEG + microalgae has occurred because of the C – O – C bond with carbohydrate of polysaccharides and carboxylic acid. The shift of absorption peak in H – C – H in wavenumber of  $1465.90 \text{ cm}^{-1}$  and  $2885.51 \text{ cm}^{-1}$  from  $\text{Fe}_3\text{O}_4$ +PEG samples has occurred due to the interaction between this sample and lipid as well as protein in microalgae.

**Table 1.** Assignment of FTIR spectra of  $\text{Fe}_3\text{O}_4$ , PEG,  $\text{Fe}_3\text{O}_4$ +PEG and  $\text{Fe}_3\text{O}_4$ +PEG+microalgae shown in Figure 2

Band	$\text{Fe}_3\text{O}_4$	PEG	$\text{Fe}_3\text{O}_4$ + PEG	$\text{Fe}_3\text{O}_4$ +PEG + microalgae
Fe – O octahedral	408.91	-	401.19	-
Fe – O tetrahedral	586.36	-	586.36	586.36
C – C	-	840.96	840.96	-
C – C	-	956.69	956.69	-
C – C	-	1056.99	1056.99	-
C – O – C	-	1103.28	1111.0	1095.57
C – O	-	1242.16	1242.16	-
C – O	-	1280.73	1280.73	-
C – O	-	1342.46	1342.46	1381.03
H – C – H	-	1465.90	1465.90	1473.62
H – C – H	-	1635.64	-	1635.64
H – C – H	-	2877.79	2885.51	2939.52
-OH	-	2893.22	2893.22	-
-OH	3433.29	3448.72	3448.72	3441.01

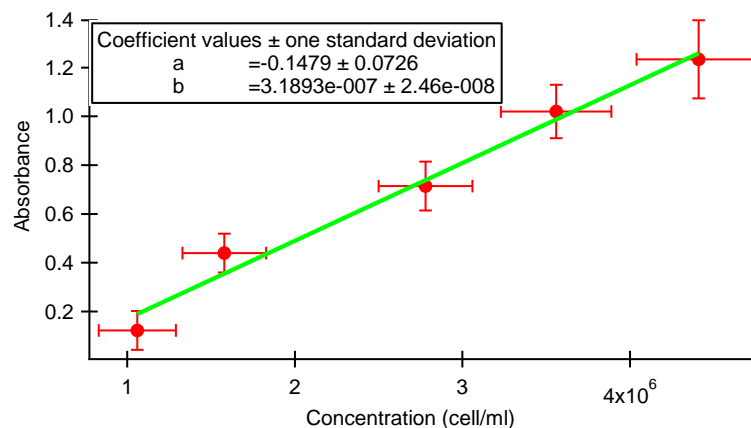
### 3.2 Calibration Curve

Figure 3 shows the relationship between concentration and absorbance for sample calibration curve.  $x$ -axis shows concentration and  $y$ -axis shows absorbance value. Based on the fitting result obtained from IGOR Pro software, linear equation is obtained as expressed in the form of  $y = bx + a$ . Error bar is obtained from standard deviation  $\Delta b$  and  $\Delta a$  that can be written as  $\Delta y = \Delta bx + \Delta a$ . From Figure 3, the relationship between the absorbance and concentration can be expressed by the following equation:

$$\text{Absorbance} = 3.19 \times 10^{-7}(\text{concentration}) - 0.14 \quad (2)$$

To determine the growth of microalgae, Equation 2 can be re-expressed as :

$$\text{Concentration} = \frac{\text{absorbance} + 0.14}{3.19 \times 10^{-7}} \quad (3)$$



**Figure 3.** Calibration curve of microalgae

### 3.3 Microalgae population growth by UV-Vis spectrophotometer

Table 2 illustrates the microalgae population that is observed by using UV-Vis spectrophotometer for 7 days. The concentration of microalgae can be determined by Equation 3. The microalgae population decreases on the second day because microalgae is still adapting to the medium. The growth of microalgae increases significantly on the third day. The growth of microalgae declines in the fourth to the seventh day and slowly begins to decline from day 4 to day 7.

**Table 2.** The growth of microalgae for 7 day observation.

Day	Absorbance	Concentration (cell/ml), $10^6$
1	$0.23 \pm 0.08$	$(1.19 \pm 0.23)$
2	$0.20 \pm 0.08$	$(1.12 \pm 0.23)$
3	$0.38 \pm 0.08$	$(1.65 \pm 0.24)$
4	$0.28 \pm 0.08$	$(1.34 \pm 0.24)$
5	$0.27 \pm 0.08$	$(1.30 \pm 0.24)$
6	$0.24 \pm 0.08$	$(1.22 \pm 0.23)$
7	$0.24 \pm 0.08$	$(1.20 \pm 0.23)$

### 3.4 Monitoring microalgae population growth by using surface plasmon resonance-based biosensor.

**3.4.1 The influence of distilled water and  $Fe_3O_4$ +PEG to the shift of SPR angle.** In this study, microalgae are detected in the form of liquid sample. Therefore, the observation of SPR phenomenon begins with observations to determine the effect of distilled water as medium for the culture of microalgae and  $Fe_3O_4$  + PEG samples as active nanoparticles to bind microalgae. The shift of SPR

angle has been occurred due to distilled water and  $\text{Fe}_3\text{O}_4$ +PEG deposition in the prism system. The red curve shows prism/Au/air system and the blue curve shows prism/Au/distilled water/cover glass (Figure 4a) and prism/Au/ $\text{Fe}_3\text{O}_4$ +PEG/cover glass (Figure 4b). The shift of SPR angle due to influence of distilled water and  $\text{Fe}_3\text{O}_4$  + PEG are 23.5 and 24.1 degrees, respectively. The  $\text{Fe}_3\text{O}_4$ +PEG has showed larger shifting of SPR angle because refractive index of  $\text{Fe}_3\text{O}_4$ +PEG is bigger than distilled water. Refractive index of  $\text{Fe}_3\text{O}_4$ +PEG is 1.63 [10] and refractive index of distilled water is 1.33[10].

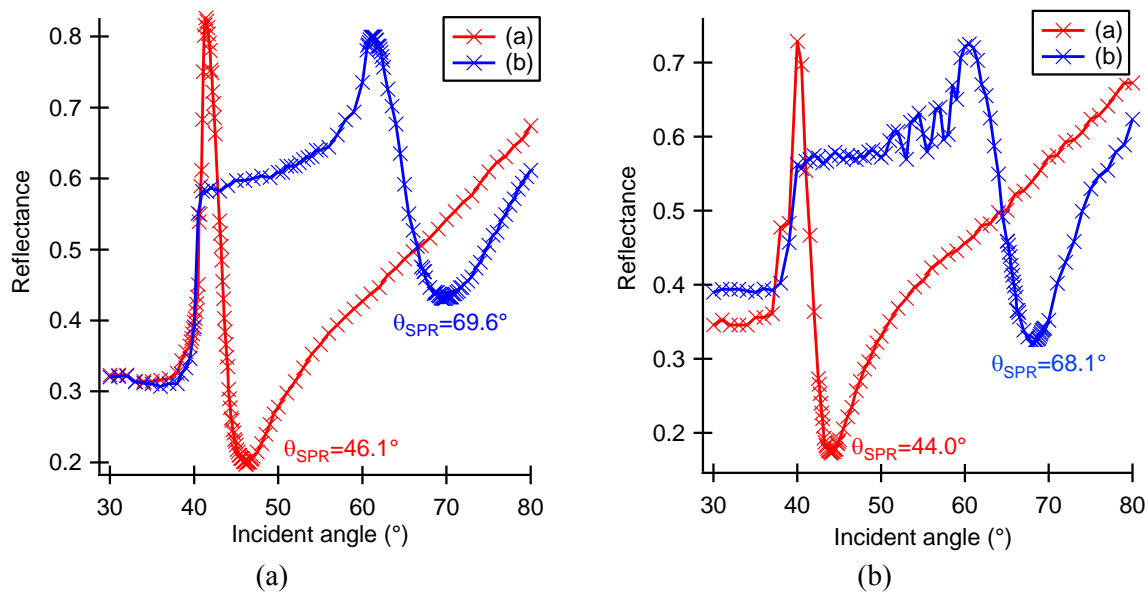


**Figure 4.** (a) The shift of SPR angle due to distilled water (b) The shift of SPR angle due to  $\text{Fe}_3\text{O}_4$ +PEG.

**3.4.2 Monitoring microalgae population growth by SPR-based biosensor.** Table 3 shows the amount of shift of SPR angle due to deposition of a mixture  $\text{Fe}_3\text{O}_4$  + PEG+microalgae. Microalgae that mixed are microalgae samples taken during the 7 days of observation using UV-Vis spectrophotometer (Table 2). Table 3 shows the response of SPR-based biosensor that is expressed by the shift of SPR angle. Prism/Au/air is initial condition (before microalgae deposition) and prism/Au/ $\text{Fe}_3\text{O}_4$ +PEG+microalgae/cover glass is SPR system after deposition  $\text{Fe}_3\text{O}_4$ +PEG+ microalgae. Based on Table 3, the shift of SPR angle is different from each other. The concentration of microalgae influences the shift of SPR angle.

**Table 3.** The shift of SPR angle for 7 days observation of microalgae.

Time (day)	Prism/Au/air	Prism/Au/ $\text{Fe}_3\text{O}_4$ +PEG+microalgae/cover glass	The shift of SPR angle ( $\Delta\theta_{\text{SPR}}$ )
1	42.8 ± 0.1	69.0 ± 0.1	26.2 ± 0.1
2	45.8 ± 0.1	70.0 ± 0.1	24.2 ± 0.1
3	43.8 ± 0.1	71.1 ± 0.1	27.3 ± 0.1
4	45.7 ± 0.1	72.8 ± 0.1	27.1 ± 0.1
5	43.6 ± 0.1	70.4 ± 0.1	26.8 ± 0.1
6	45.0 ± 0.1	71.3 ± 0.1	26.3 ± 0.1
7	44.0 ± 0.1	68.8 ± 0.1	24.8 ± 0.1

Figure 5 shows the results of monitoring the growth of microalgae with SPR based biosensor and UV-Vis spectrophotometer. The blue line shows the respon of SPR based biosensor based on the shift

in SPR angle, while the red line shows the microalgae growth charts derived from UV-Vis spectrophotometer. The growth of microalgae with SPR-based biosensor shows the same pattern graphics as indicated by UV-Vis spectrophotometer. Therefore, SPR-based biosensors have the potential to be further developed for monitoring the growth of microalgae so that the process of monitoring the growth of microalgae is more effective and has the potential to be monitored in real time.

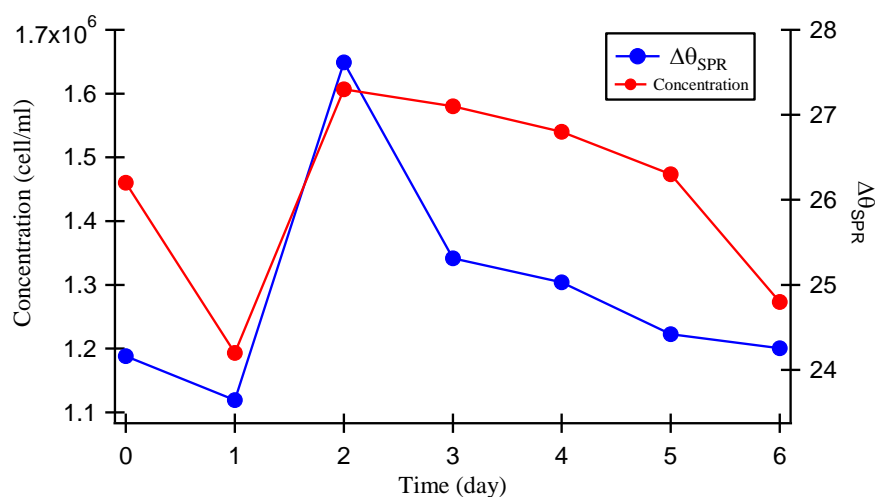


**Figure 5.** Growth monitoring of microalgae by using SPR based biosensor and UV-Vis spectrophotometer.

#### 4. Conclusions

$\text{Fe}_3\text{O}_4$  nanoparticles have been successfully functionalized by PEG-4000 for monitoring of microalgae. It is proven by the discovery of interaction between  $\text{Fe}_3\text{O}_4$  + PEG-4000 with components of microalgae which consists of carbohydrates, protein, carboxyl group and lipid in the FTIR spectra. The microalgae population growth has been successfully monitored by using a SPR-based biosensor. Finally, the shift of SPR angle can be used for monitoring the microalgae population growth.

#### 5. References

- [1] Raether P D H 1988 Surface plasmons on smooth surfaces *Surface Plasmons on Smooth and Rough Surfaces and on Gratings* Springer Tracts in Modern Physics (Springer Berlin Heidelberg) pp 4–39
- [2] Islam M S and Kouzani A Z 2013 Simulation and Analysis of a Sub-Wavelength Grating Based Multilayer Surface Plasmon Resonance Biosensor *J. Light. Technol.* **31** 1388–98
- [3] Yang D, Lu H-H, Chen B and Lin C-W 2010 Surface Plasmon Resonance of  $\text{SnO}_2/\text{Au}$  Bi-layer Films for Gas Sensing Applications *Sens. Actuators B Chem.* **145** 832–8
- [4] Linman M J, Sugerman K and Cheng Q 2010 Detection of low levels of *Escherichia coli* in fresh spinach by surface plasmon resonance spectroscopy with a TMB-based enzymatic signal enhancement method *Sens. Actuators B Chem.* **145** 613–619
- [5] Mazumdar S D, Barlen B, Kämpfer P and Keusgen M 2010 Surface plasmon resonance (SPR) as a rapid tool for serotyping of *Salmonella* *Biosens. Bioelectron.* **25** 967–971
- [6] Chabot V, Cuerrier C M, Escher E, Aimez V, Grandbois M and Charette P G 2009 Biosensing based on surface plasmon resonance and living cells *Biosens. Bioelectron.* **24** 1667–1673
- [7] Jafari A, Shayesteh S F, Salouti M and Boustani K 2015 Effect of annealing temperature on magnetic phase transition in  $\text{Fe}_3\text{O}_4$  nanoparticles *J. Magn. Magn. Mater.* **379** 305–312
- [8] Sun J, Zhou S, Hou P, Yang Y, Weng J, Li X and Li M 2007 Synthesis and characterization of biocompatible  $\text{Fe}_3\text{O}_4$  nanoparticles *J. Biomed. Mater. Res. A* **80** 333–341

- [9] Duygu D Y, Udoh A U, Ozer T B, Akbulut A, Erkaya I A, Yildiz K and Guler D 2012 Fourier transform infrared (FTIR) spectroscopy for identification of *Chlorella vulgaris* Beijerinck 1890 and *Scenedesmus obliquus* (Turpin) Kützing 1833 *Afr. J. Biotechnol.* **11** 3817–3824
- [10] Hale G M and Querry M R 1973 Optical constants of water in the 200-nm to 200- $\mu$ m wavelength region *Appl. Opt.* **12** 555–563

### **Acknowledgments**

The reported paper was financially supported by *Hibah Kompetensi* (HIKOM) from the Ministry of research and Technology of High Education for the period of 2015- 2017 and thesis scholarship of *Lembaga Pengolahan Dana Pendidikan* (LPDP) batch 3 for the period of 2016.